

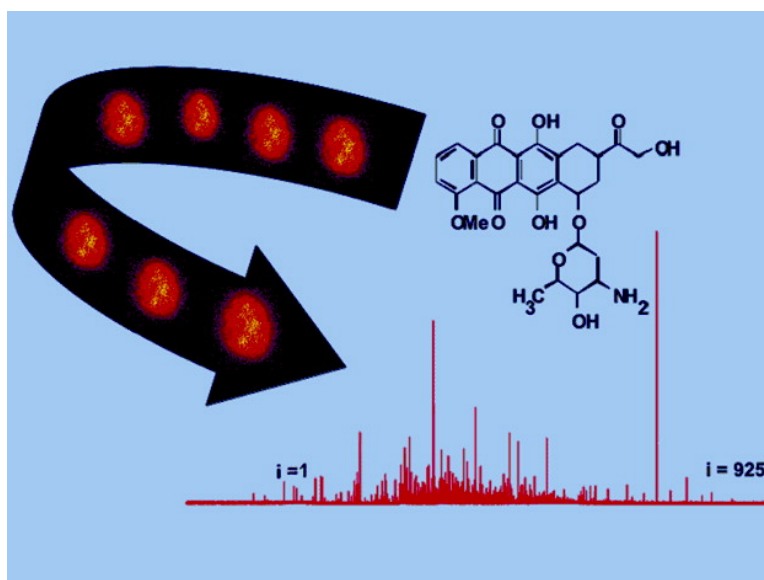
Communication

Doxorubicin Accumulation in Individually Electrophoresed Organelles

Adrian B. Anderson, Guohua Xiong, and Edgar A. Arriaga

J. Am. Chem. Soc., **2004**, 126 (30), 9168-9169 • DOI: 10.1021/ja0492539 • Publication Date (Web): 09 July 2004

Downloaded from <http://pubs.acs.org> on April 1, 2009



More About This Article

Additional resources and features associated with this article are available within the HTML version:

- Supporting Information
- Access to high resolution figures
- Links to articles and content related to this article
- Copyright permission to reproduce figures and/or text from this article

[View the Full Text HTML](#)



ACS Publications
 High quality. High impact.

Doxorubicin Accumulation in Individually Electrophoresed Organelles

Adrian B. Anderson, Guohua Xiong, and Edgar A. Arriaga*

Department of Chemistry, University of Minnesota, Minneapolis, Minnesota 55455

Received February 11, 2004; E-mail: arriaga@chem.umn.edu

Subcellular drug distribution plays an important role in drug efficacy and cell cytotoxicity.^{1,2} For instance, the accumulation of doxorubicin (DOX, Figure 1), a widely used chemotherapeutic compound, in mitochondria has been associated with DOX cytotoxicity.^{3,4} How DOX is distributed among hundreds of mitochondria found in a cell is still unknown. New bioanalytical approaches reporting on individual organelle drug content may help characterize the heterogeneity found in subcellular accumulation of drugs such as DOX. This report capitalizes on individual organelle measurements to investigate the DOX distribution in mitochondria.

Using capillary electrophoresis with laser-induced fluorescence detection (CE-LIF) mitochondria are separated as has been described previously.^{5,6} The unique electrophoretic mobility of each organelle causes migration of each organelle toward the LIF detector (Figure 1) at different speeds. When an organelle leaves the separation capillary (I) and travels through a focused laser beam (J), its fluorescence is selected with two interference filters, (E) and (G), that are spectrally selective for DOX native fluorescence and the emission of MitoTracker Green (MTG), respectively. The latter is a fluorescent probe commonly used to identify mitochondria.

Figure 2 is part of a dual-trace electropherogram resulting from the analysis of an MTG-stained organelle fraction isolated from DOX-treated CCL-119 cells. Peaks in both traces were assigned to mitochondria containing DOX (e.g., peak a, Figure 2A), unless the ratio of the peak intensities at 635 and 510 nm was less than the spectral cross-talking factor (i.e. $<0.07 \pm 0.02$ [average \pm SD, $n = 218$]), an indication that a mitochondrion either contains no DOX or amounts below the detectable range (e.g., peak b, Figure 2A). An interesting example is the doublet c (Figure 2A) that shows one mitochondrion without any detectable DOX content followed by a second DOX-containing mitochondrion. Organelles other than mitochondria containing DOX were also detected (e.g., peak d, Figure 2B). These assignments are based on the results from controls consisting of no treatment or DOX or MTG treatment alone (see Supporting Information). These events do not correspond to DOX or MTG diffusing in solution during the electrophoretic separation because that would have led to the detection of broad peaks (~ 2 s) rather than a narrow peak ($\sim 90 \pm 20$ ms).

A summary of the classification of detected organelles based on the detection criterion outlined above is presented in Table 1. This tabulation includes data from organelles isolated from CEM/C2 (drug resistant) and CCL-119 (drug sensitive) cell lines, subject to both DOX-treatment and MTG-staining. These data indicate that (i) only a fraction of mitochondria contain DOX at detectable levels (17.0% and 9.4%, CEM/C2 and CCL-119 cell lines, respectively, Table 1) which is indicative of heterogeneity in mitochondria; (ii) there is a statistical difference in the abundance of DOX-containing mitochondria between the two cell lines (see Supporting Information). The presence of other DOX-containing organelles in the organellar fractions (7.2% CEM/C2 and 4.6% CCL-119) is also

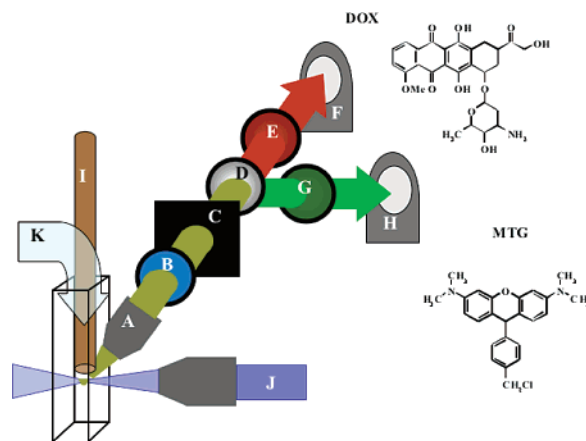


Figure 1. CE-LIF detection scheme for doxorubicin (DOX) and MitoTracker green (MTG). Collection objective (A); 505 nm LP laser filter (B); pinhole (C); 580 nm LP dichroic mirror (D); 635 ± 27.5 nm filter (E); PMT for DOX detection (F); 510 ± 20 nm filter (G); PMT for MTG detection (H); AAP-coated separation capillary (I); 488 nm argon ion laser (J); sheath flow (K).

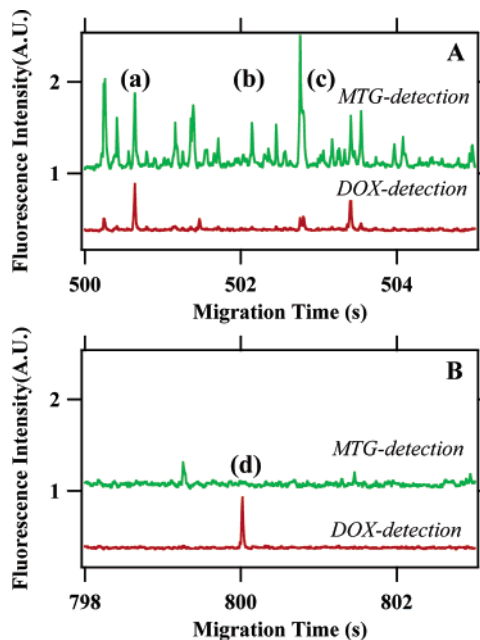


Figure 2. CE-LIF detection of organelles isolated from CCL-119 cells. Only 5-s time windows are shown. MTG detection was at 510 ± 20 nm, DOX detection was at 635 ± 27.5 nm. Panel A shows examples of a mitochondrion containing DOX (a), mitochondrion with no or low levels of DOX (b), and two mitochondria without and with DOX (c). Panel B shows an organelle that is not a mitochondrion containing DOX (d). Separation was carried out at -300 V/cm using 210 mM sucrose, 10 mM HEPES (pH 7.4) as separation buffer. See Supporting Information.

expected because these fractions are known to contain other organelles that can accumulate DOX (i.e., acidic organelles).⁷

Table 1. Classification of Detected Organelles

cell line	detected fraction (%) ^a			N	LL ^b	UL ^c	Mn ^b
	DOX	MTG	both				
CEM/C2	7.2	75.8	17.0	3680	22	8.2	51
CCL119	4.6	86.0	9.4	2068	26	43	54

^a Column entries correspond to peaks detected only at 635 nm (DOX), only at 510 nm (MTG), and both nominal wavelengths, respectively. ^b Units are zmol. ^c Units are amol. N: number of detected events. LL: lower limit. UL: upper limit. Mn: median.

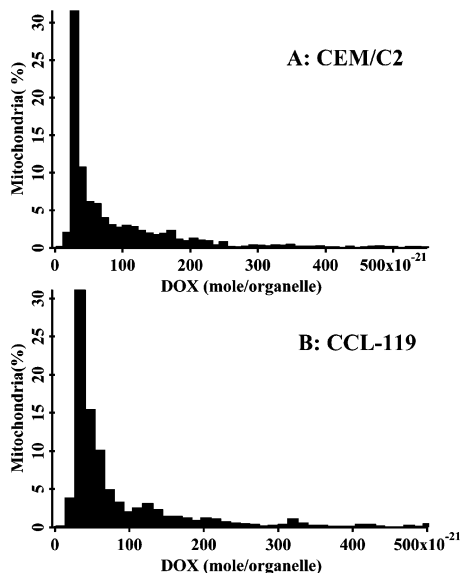


Figure 3. DOX content in individual mitochondria: organelles were isolated from DOX-treated CEM/C2 (Panel A) and DOX-treated CCL-119 cells (Panel B). Treatment: 10 μ M DOX for 12 h.

To estimate the amount of DOX per mitochondrion, the LIF detector response to DOX in mitochondria was determined in a parallel experiment (see Supporting Information). The DOX content of an individual mitochondrion (m , moles) was calculated as $m = (1.07 \times 10^{-18}) \times h$, where h is the peak height of an individual mitochondrion (e.g., peak a, DOX detection, Figure 2A), and a proportionality constant (1.07×10^{-18}) [mol/au]. Figure 3 presents normalized histograms of the DOX content of the individual mitochondria isolated from the CEM/C2 and CCL-119 cell lines. The wide range of DOX per mitochondrion spanning 2 orders of magnitude (Table 1) points to heterogeneity in the DOX content of individual mitochondria. The effect of mitochondrial fragmentation or aggregation on the observed range is minimal because of the gentle preparation procedures and the highly diluted samples used in these studies (See Supporting Information). The distributions

shown in Figure 3 have median values of 51 and 54 zmol DOX per mitochondrion for CEM/C2 and CCL-119 cells, respectively (cf. Table 1). These DOX amounts are 2 orders of magnitude higher than would be expected if DOX used in the treatment (10 μ M) simply diffused into the 50-aL volume of an average mitochondrion. Interactions of DOX with molecules found in the mitochondrion such as cardiolipin ($K = 1.8 \times 10^6 \text{ M}^{-1}$),⁸ DNA ($K = 3.6 \times 10^6 \text{ M}^{-1}$),⁸ and cytochrome c ⁹ are likely enhancing the accumulation of this cancer drug in this subcellular environment. Mitochondrial membrane potential may also serve as a driving force for the accumulation of DOX in mitochondria.¹⁰

The results presented here suggest that the subcellular localization of fluorescent compounds in individual organelles is quantifiable by CE-LIF. The high accumulation of DOX in mitochondria presents an example in which these measurements reveal a new dimension in heterogeneity at the subcellular level and points to the presence of underlying mechanisms leading to the accumulation of this drug. Other cancer drugs, other preparations of DOX (i.e., Doxil, a liposomal DOX preparation), or other organelles (e.g., acidic organelles) detectable by LIF, could also be investigated using this approach. Determining DOX distributions in individual mitochondria from tissues (i.e., heart) from subjects treated with this drug may reveal the relevance of mitochondrial heterogeneity in DOX toxicity.

Acknowledgment. DOX was donated by A. Suarato. Statistical analysis was done by H. Ahmadzadeh and Y. Chen. NIH R01-GM61969 supports this work. E.A. is an NIH Career Award Fellow (1K02-AG21453).

Supporting Information Available: Experimental protocols. This material is available free of charge via the Internet at <http://pubs.acs.org>.

References

- (1) Abdella, B. R. J.; Fisher, J. *Environ. Health Perspect.* **1985**, *64*, 3–18.
- (2) Kiyomiya, K.; Matsuo, S.; Kurebe, M. *Cancer Chemother. Pharmacol.* **2001**, *47*, 51–56.
- (3) Zhou, S. Y.; Starkov, A.; Frober, M. K.; Leino, R. L.; Wallace, K. B. *Cancer Res.* **2001**, *61*, 771–777.
- (4) Singh, K. K.; Russell, J.; Sigala, B.; Zhang, Y. G.; Williams, J.; Keshav, K. F. *Oncogene* **1999**, *18*, 6641–6646.
- (5) Duffy, C. F.; McEathron, A. A.; Arriaga, E. A. *Electrophoresis* **2002**, *23*, 2040–2047.
- (6) Duffy, C. F.; Fuller, K. M.; Malvey, M. W.; O’Kennedy, R.; Arriaga, E. A. *Anal. Chem.* **2002**, *74*, 171–176.
- (7) Radko, S. P.; Stastna, M.; Chrambach, A. *Anal. Chem.* **2000**, *72*, 5955–5960.
- (8) Altan, N.; Chen, Y.; Schindler, M.; Simon, S. M. *J. Exp. Med.* **1998**, *187*, 1583–1598.
- (9) Goormaghtigh, E.; Chatelain, P.; Caspers, J.; Ruysschaert, J. M. *Biochim. Biophys. Acta* **1980**, *29*, 3003–3010.
- (10) Papadopoulou, L. C.; Theophilidis, G.; Thomopoulos, G. N.; Tsiftoglou, A. S. *Biochem. Pharmacol.* **1999**, *57*, 481–489.
- (11) Xu, M. F.; Ashraf, M. *J. Mol. Cell. Cardiol.* **2002**, *34*, 75–79.

JA0492539